SOI: 1.1/TAS DOI: 10.15863/TAS

International Scientific Journal

Theoretical & Applied Science

p-ISSN: 2308-4944 (print) **e-ISSN:** 2409-0085 (online)

Year: 2023 **Issue:** 02 **Volume:** 118

Published: 07.02.2023 **http://T-Science.org**

Issue Article

Denis Chemezov
Vladimir Industrial College
M.Sc.Eng., Academician of International Academy of
Theoretical and Applied Sciences, Lecturer, Russian Federation
https://orcid.org/0000-0002-2747-552X
vic-science@yandex.ru

Agannes Arzikyan
Vladimir Industrial College
Student, Russian Federation

Pyotr German
Moscow Aviation Institute (NRU)
Branch in Zhukovsky, Moscow Oblast,
Student, Russian Federation

Dmitriy Bychkov
Vladimir Industrial College
Student, Russian Federation

Danil Sukhorukov
Vladimir Industrial College
Student, Russian Federation

Maksim Perov
Vladimir Industrial College
Student, Russian Federation

Sergey Lukashov
Vladimir State University named after Alexander & Nikolay Stoletovs
Institute of Mechanical Engineering & Automobile Transport
Student, Russian Federation

REFERENCE DATA OF PRESSURE DISTRIBUTION ON THE SURFACES OF AIRFOILS HAVING THE NAMES BEGINNING WITH THE LETTER P

Abstract: *The results of the computer calculation of air flow around the airfoils having the names beginning with the letter P are presented in the article. The contours of pressure distribution on the surfaces of the airfoils at angles of attack of 0, 15 and -15 degrees in conditions of the subsonic airplane flight speed were obtained.*

Key words: *airfoil, angle of attack, pressure, surface.*
Language: *English*
Citation: Chemezov, D., et al. (2023). Reference data of pressure distribution on the surfaces of airfoils having the names beginning with the letter P. *ISJ Theoretical & Applied Science, 02 (118),* 48-61.
Soi: http://s-o-i.org/1.1/TAS-02-118-9 ***Doi***: crossref https://dx.doi.org/10.15863/TAS.2023.02.118.9
Scopus ASCC: *1507.*

Introduction

Creating reference materials that determine the most accurate pressure distribution on the airfoil surfaces is an actual task of the airplane aerodynamics.

Materials and methods

The study of air flow around the airfoils was carried out in a two-dimensional formulation by means of the computer calculation in the *Comsol Multiphysics* program. The airfoils in the cross section were taken as objects of research [1-32]. In this work, the airfoils having the names beginning with the letter *P* were adopted. Air flow around the airfoils was carried out at angles of attack (α) of 0, 15 and -15 degrees. Flight speed of the airplane in each case was subsonic. The airplane flight in the atmosphere was carried out under normal weather conditions. The geometric characteristics of the studied airfoils are presented in the Table 1. The geometric shapes of the airfoils in the cross section are presented in the Table 2.

Table 1. The geometric characteristics of the airfoils.

Airfoil name	Max. thickness	Max. camber	Leading edge radius	Trailing edge thickness
P50-3	9.7% at 20.0% of the chord	9.5% at 50.0% of the chord	1.1731%	0.0%
P-51D ROOT (BL17,5)	16.52% at 38.9% of the chord	1.26% at 68.3% of the chord	1.6258%	0.0%
P-51D TIP (BL215)	11.42% at 46.3% of the chord	1.3% at 46.3% of the chord	0.4064%	0.0%
Pegase coap	17.36% at 34.3% of the chord	3.65% at 31.1% of the chord	2.8912%	0.268%
Phoenix	8.19% at 27.5% of the chord	2.78% at 25.0% of the chord	0.3739%	0.252%
PIATTELL	15.21% at 20.0% of the chord	7.82% at 30.0% of the chord	2.672%	0.0%
Piattelli C1	15.47% at 25.0% of the chord	7.82% at 30.0% of the chord	2.8693%	0.0%
pmc19sm	9.19% at 34.2% of the chord	2.12% at 17.5% of the chord	0.5464%	0.198%
PRD 2	12.97% at 30.0% of the chord	6.73% at 40.0% of the chord	1.805%	0.0%
PRD 3	13.63% at 30.0% of the chord	7.2% at 40.0% of the chord	2.0895%	0.0%
PRD 4	12.48% at 30.0% of the chord	6.24% at 30.0% of the chord	1.2478%	0.0%
Profil 374 Dicke 10,92%	10.9% at 36.2% of the chord	2.23% at 41.3% of the chord	0.6706%	0.0%
Profil 387 Dicke 9,06%	9.03% at 28.9% of the chord	3.79% at 39.3% of the chord	0.6641%	0.0%
PROFILE12A 9,00%	8.99% at 34.4% of the chord	1.8% at 34.4% of the chord	0.5536%	0.0%
PROPFAN CRUISE MISSILE WING	8.19% at 40.0% of the chord	1.33% at 50.0% of the chord	0.3085%	0.261%
PSU 90-1	12.53% at 34.1% of the chord	2.43% at 49.5% of the chord	0.9386%	0.0%
PSU-90-125WL	12.53% at 34.1% of the chord	2.43% at 49.5% of the chord	0.9386%	0.0%
PT40	11.59% at 27.1% of the chord	2.88% at 41.6% of the chord	3.7397%	0.2704%
PWINGLET	12.58% at 34.2% of the chord	2.44% at 49.7% of the chord	1.1175%	0.044%

Note:
Piattelli C1 (F. Piattelli (Italy));
PRD 2, PRD 3, PRD 4 (G. Dorio (Italy)).

Table 2. The geometric shapes of the airfoils in the cross section.

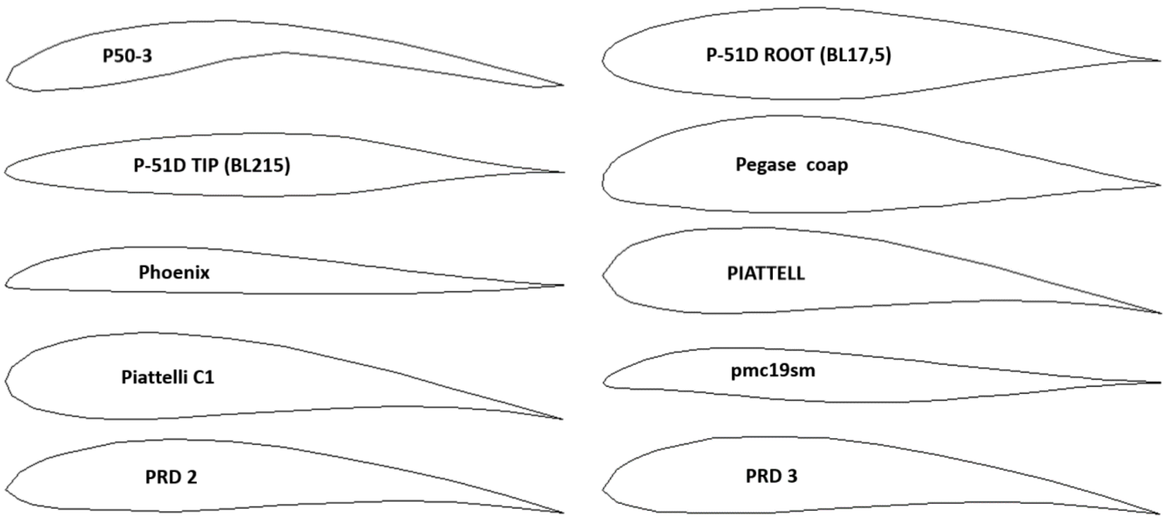

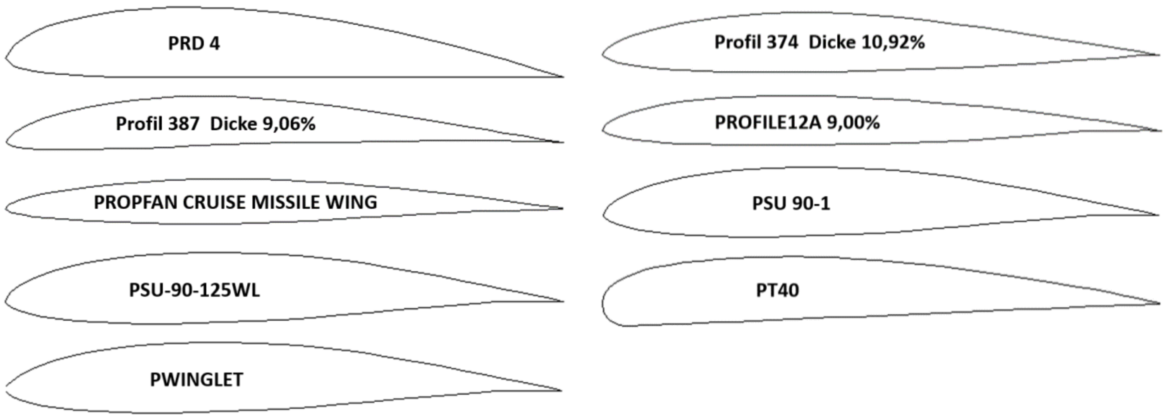

Results and discussion

The calculated pressure contours on the surfaces of the airfoils at different angles of attack are presented in the Figs. 1-19. The calculated values on the scale can be represented as the basic values when comparing the pressure drop under conditions of changing the angle of attack of the airfoils.

19 airfoils of various configurations were considered. A common characteristic of all airfoils was that they were asymmetrical.

It can also be noted that the maximum thickness of the airfoil was determined for Pegase coap, and the minimum thickness was determined for Phoenix and PROPFAN CRUISE MISSILE WING. At the same time, it should be noted that the greatest thickness values were determined up to the middle of the length of the airfoil in the cross section from the leading edge.

The maximum and minimum camber values of the airfoils are 9.5% and 1.26% for P50-3 and P-51D ROOT (BL17,5), respectively.

The largest and smallest leading edge radii of 3.7397% and 0.3085% were also determined for the PT40 and PROPFAN CRUISE MISSILE WING airfoils, respectively.

The trailing edge thickness for most of the considered airfoils is 0.0%. The maximum trailing edge thickness was determined for the PT40 airfoil.

Applying the geometric characteristics of the airfoils analyzed above, we will compare the results of computer calculations to determine the aerodynamic characteristics of the wings in conditions of horizontal flight and maneuvers of the airplane.

High drag values reduce the aerodynamic characteristics of the airplane wing. Therefore, it is necessary to analyze the maximum and minimum calculated values of pressures on the leading edge of the airfoils exposed to intense air flows at angles of attack of 0, 15 and -15 degrees.

Pressure in a small range from 6.43 to 6.6 kPa is created on the leading edge of the airfoils during horizontal flight. At the same time, the most favorable flight conditions were determined for the Phoenix airfoil.

During the airplane climb, large negative pressures act on the upper part of the leading edge of the airfoils. The pressure value varies in the range from -15.3 to -79.1 kPa. The higher pressure values act on the leading edge of thin and medium-thick airfoils. However, the PROPFAN CRUISE MISSILE WING airfoil demonstrates good aerodynamic characteristics during the airplane climb. This airfoil is an exception to the above conclusion. Maximum design pressure is subjected to the PROFILE12A 9,00% airfoil.

Large negative pressures act on the lower part of the leading edge of the airfoils during the airplane descent. The pressure value varies in the range from -9.62 to -64.4 kPa. Thus, it can be concluded that during the airplane descent, the wings are subjected to pressure on average 38% less than during climb. The Profil 387 Dicke 9,06% airfoil demonstrates good aerodynamic characteristics during the airplane descent. The maximum design pressure is subjected to the PWINGLET airfoil.

Based on the analysis carried out, it is possible to draw a conclusion on this chapter. The medium-thick and small values of the radii of the airfoils, such as PROPFAN CRUISE MISSILE WING and Profil 387 Dicke 9,06%, contribute to the reduction of drag.

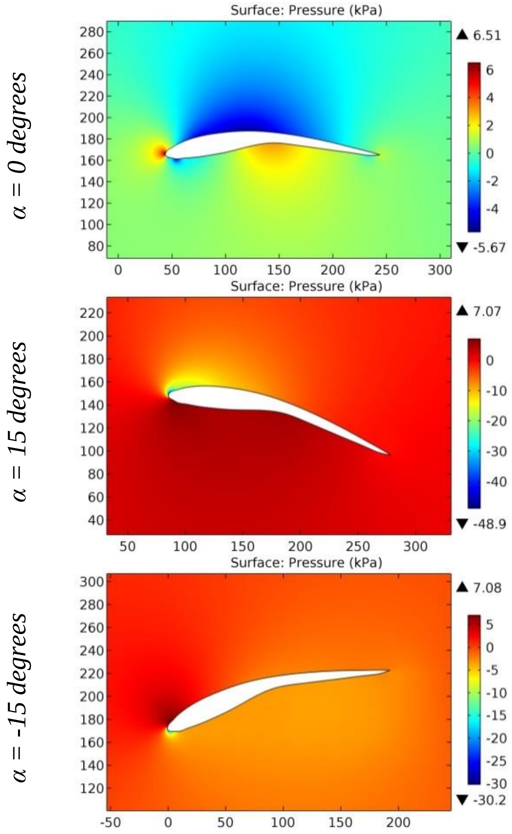

Figure 1. The pressure contours on the surfaces of the P50-3 airfoil.

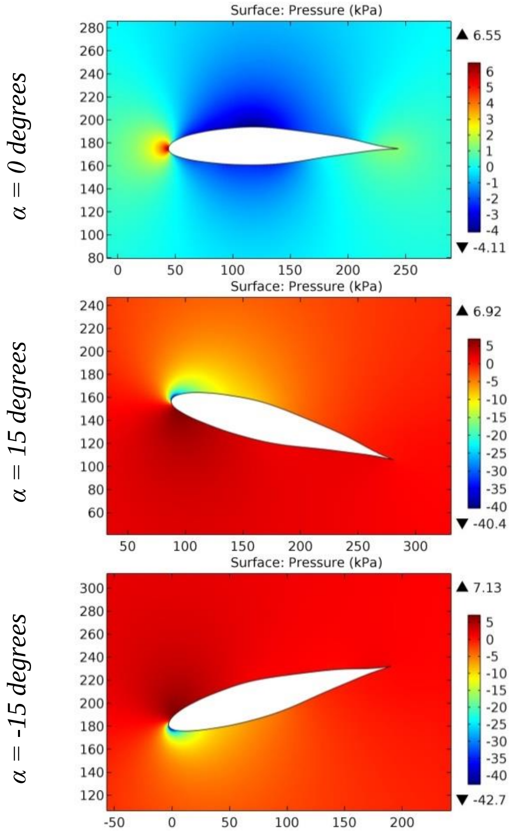

Figure 2. The pressure contours on the surfaces of the P-51D ROOT (BL17,5) airfoil.

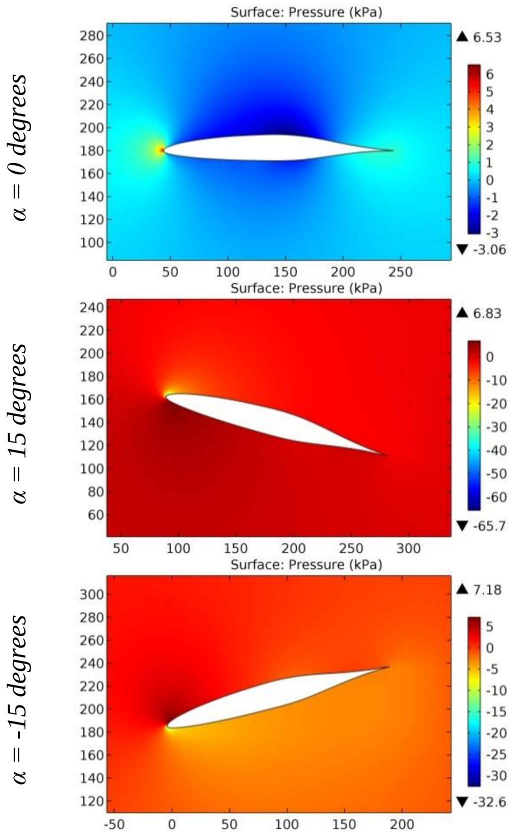

Figure 3. The pressure contours on the surfaces of the P-51D TIP (BL215) airfoil.

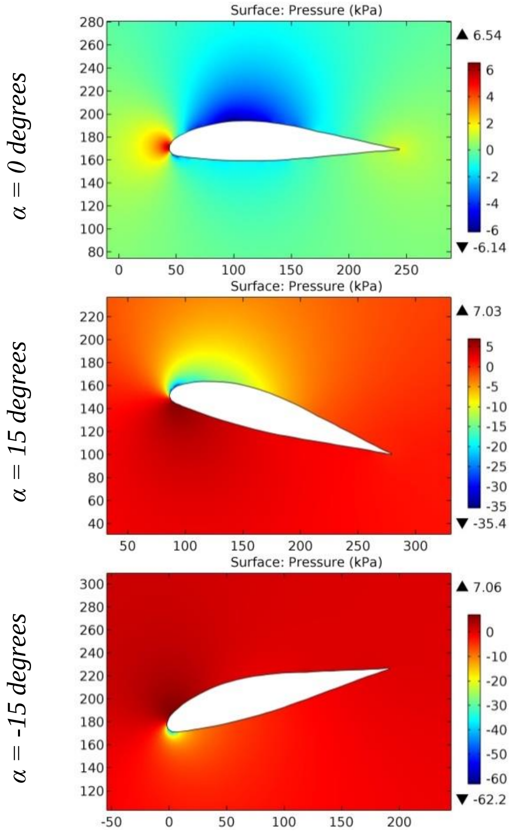

Figure 4. The pressure contours on the surfaces of the Pegase coap airfoil.

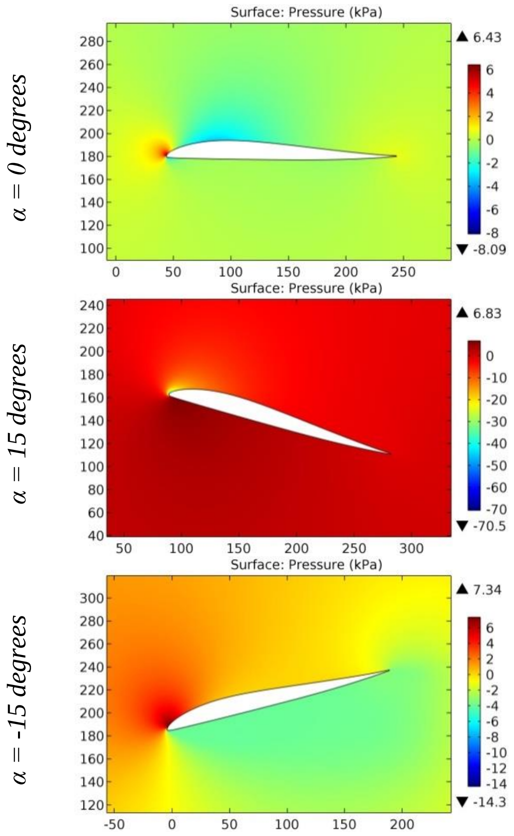

Figure 5. The pressure contours on the surfaces of the Phoenix airfoil.

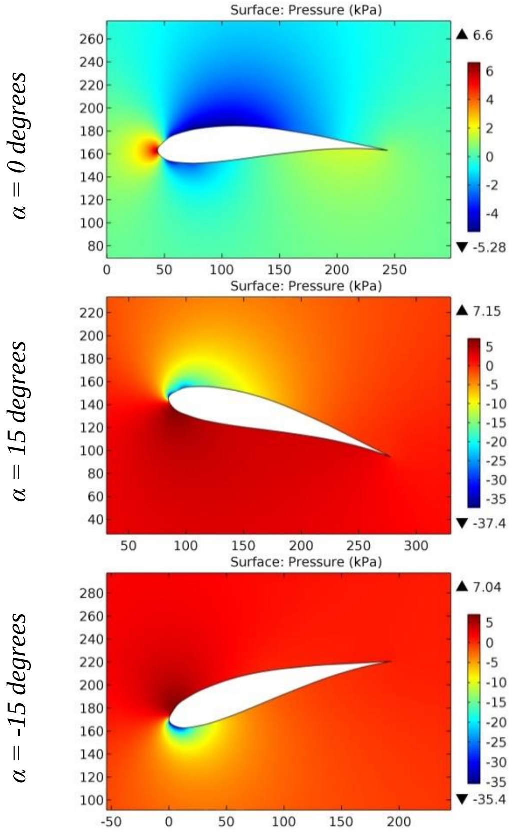

Figure 6. The pressure contours on the surfaces of the PIATTELL airfoil.

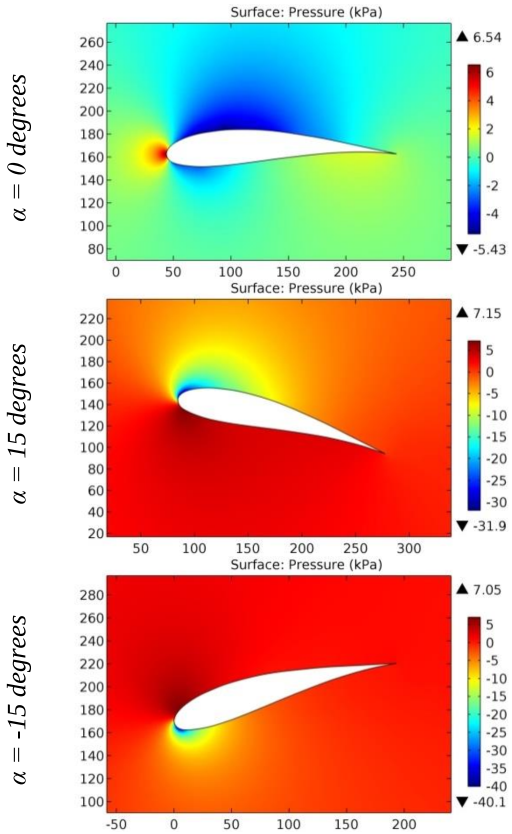

Figure 7. The pressure contours on the surfaces of the Piattelli C1 airfoil.

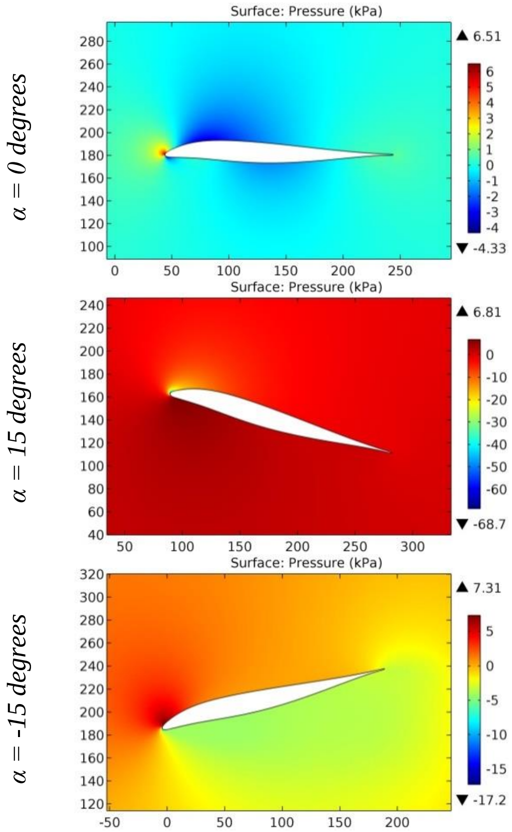

Figure 8. The pressure contours on the surfaces of the pmc19sm airfoil.

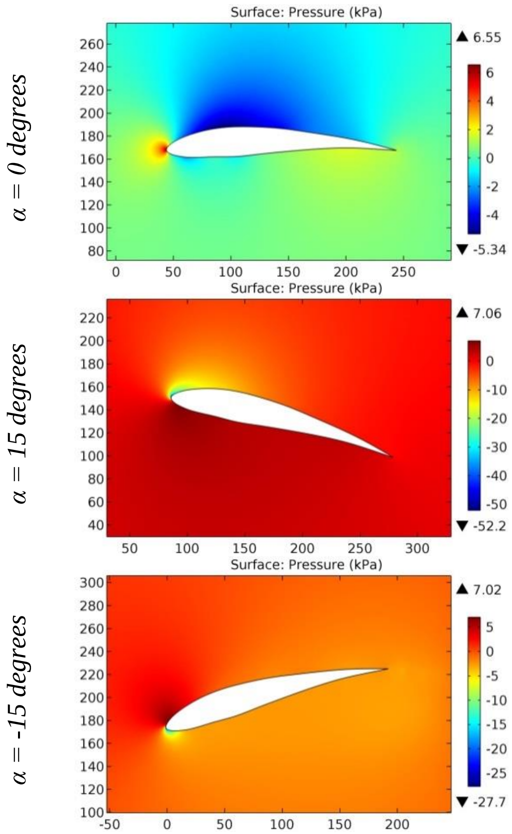

Figure 9. The pressure contours on the surfaces of the PRD 2 airfoil.

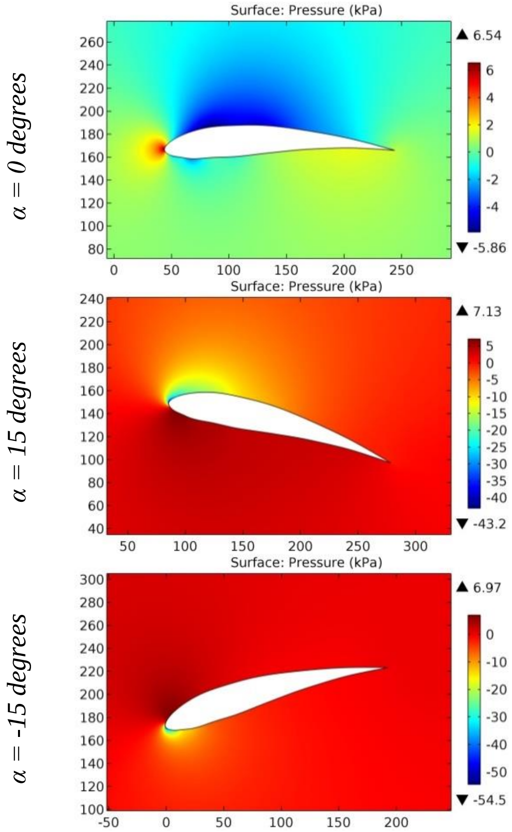

Figure 10. The pressure contours on the surfaces of the PRD 3 airfoil.

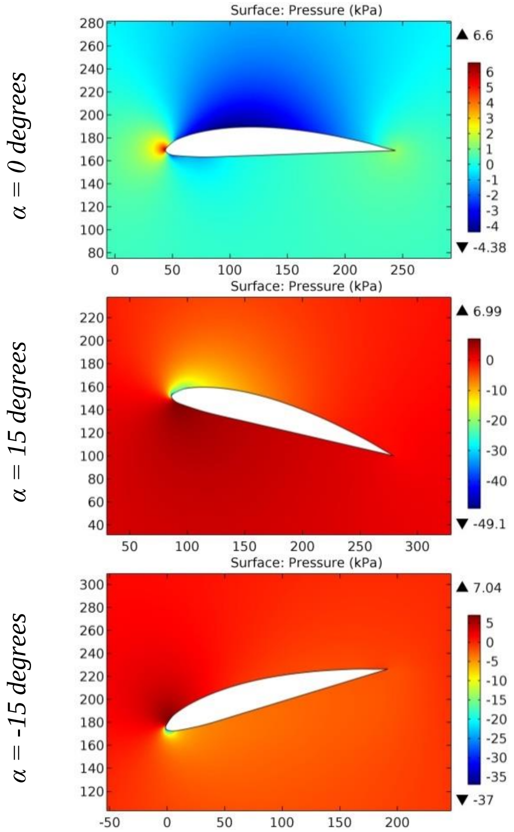

Figure 11. The pressure contours on the surfaces of the PRD 4 airfoil.

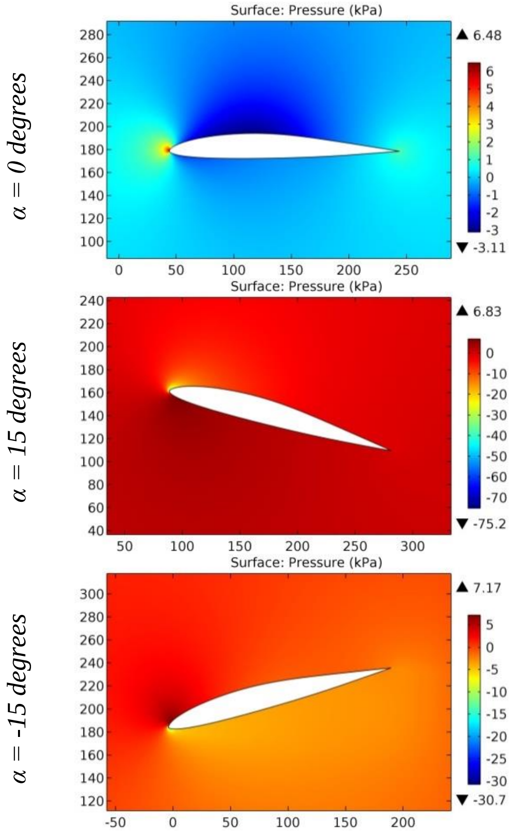

Figure 12. The pressure contours on the surfaces of the Profil 374 Dicke 10,92%.

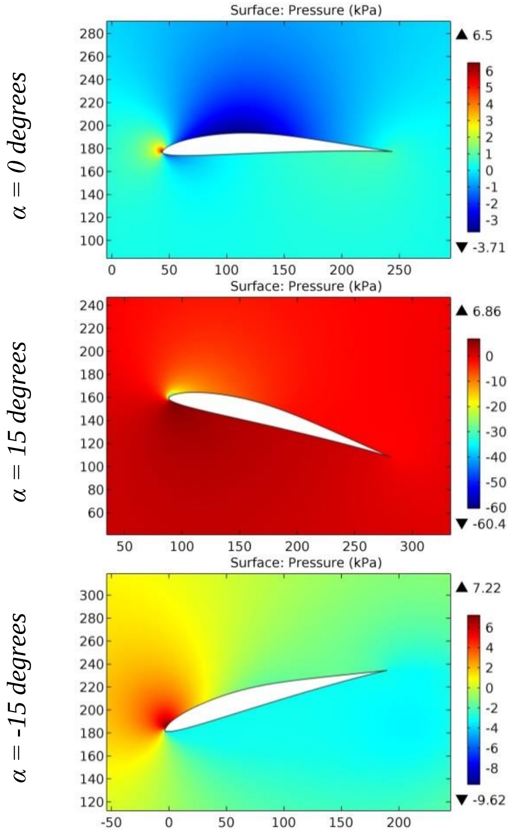

Figure 13. The pressure contours on the surfaces of the Profil 387 Dicke 9,06%.

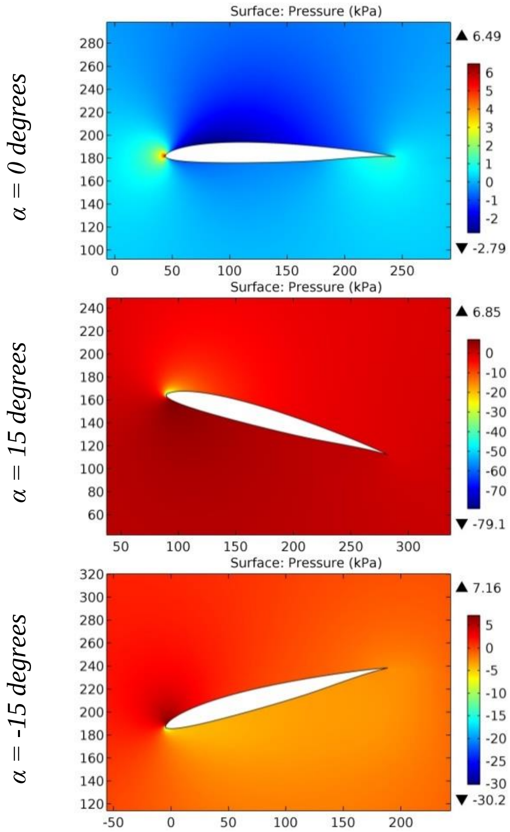

Figure 14. The pressure contours on the surfaces of the PROFILE12A 9,00%.

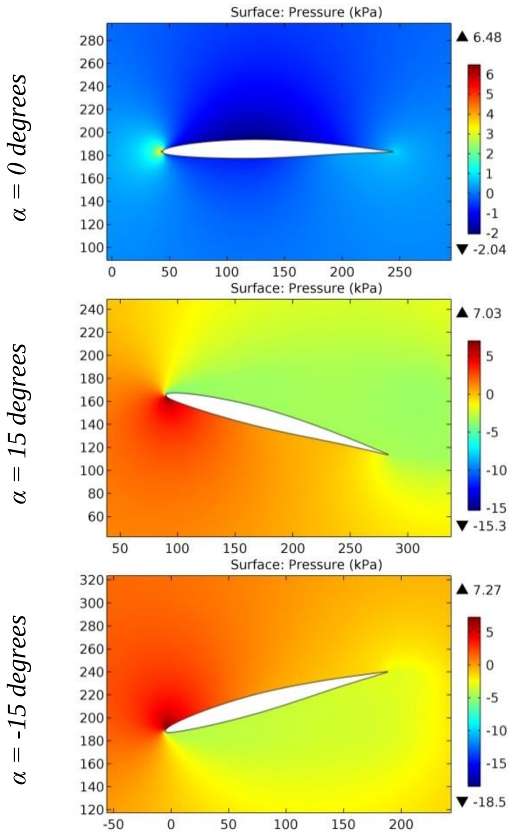

Figure 15. The pressure contours on the surfaces of the PROPFAN CRUISE MISSILE WING.

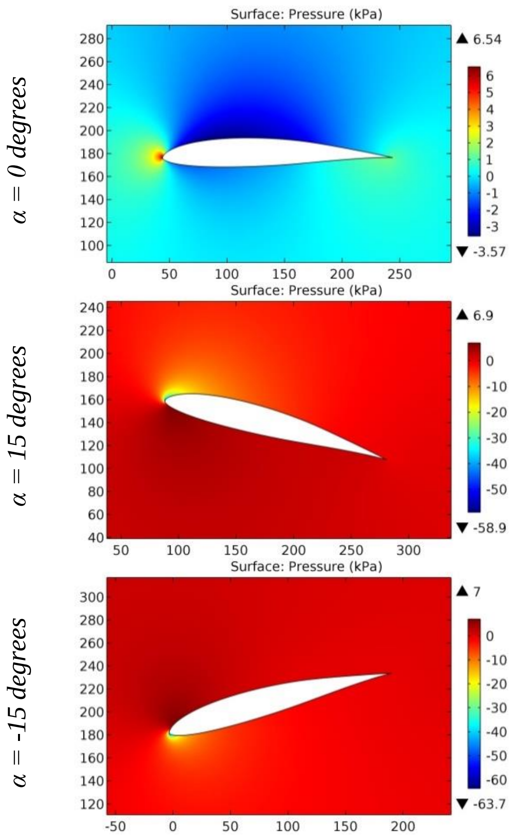

Figure 16. The pressure contours on the surfaces of the PSU 90-1 airfoil.

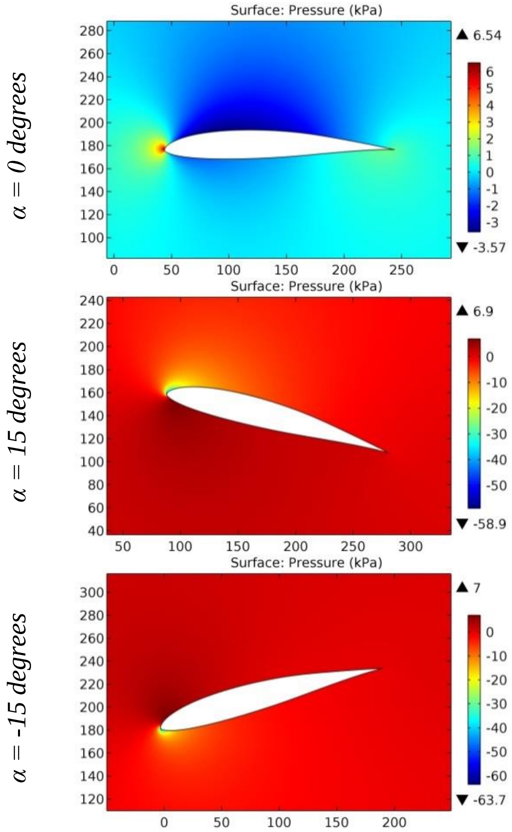

Figure 17. The pressure contours on the surfaces of the PSU-90-125WL airfoil.

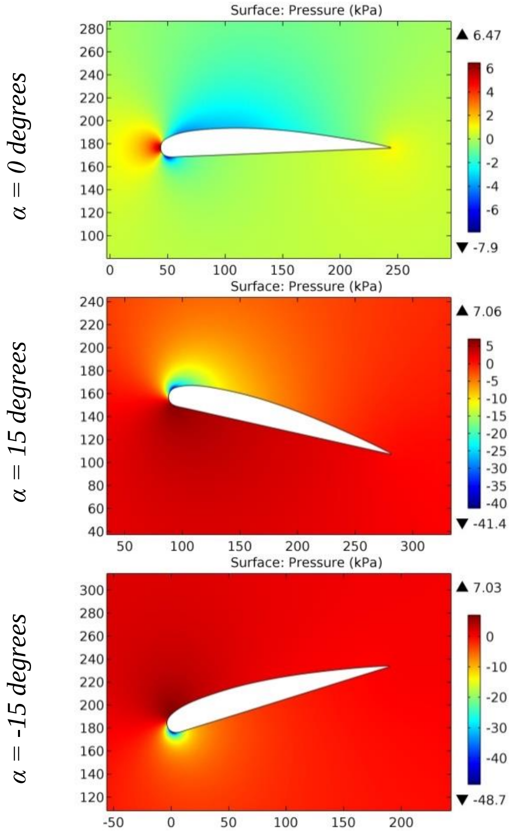

Figure 18. The pressure contours on the surfaces of the PT40 airfoil.

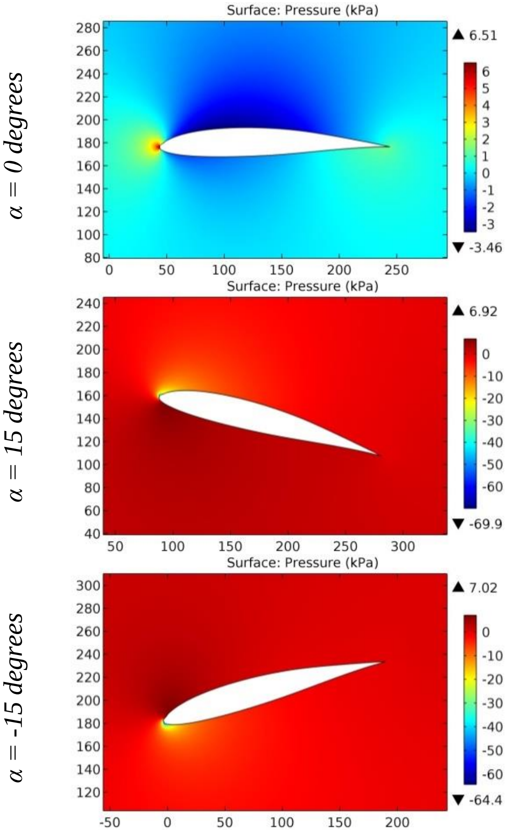

Figure 19. The pressure contours on the surfaces of the PWINGLET airfoil.

Conclusion

According to the pressure distribution gradients calculated in a two-dimensional formulation, it is possible to imagine the nature of resistance of the edges and surfaces of airfoils of the wings in the air flow during the airplane movement. Analysis of the calculated values of pressures on the leading edge showed that thin and medium-thick airfoils are subjected to greater drag during climb than during descent with a similar geometry of the wing in the cross section.

References:

1. Anderson, J. D. (2010). *Fundamentals of Aerodynamics.* McGraw-Hill, Fifth edition.
2. Shevell, R. S. (1989). *Fundamentals of Flight.* Prentice Hall, Second edition.
3. Houghton, E. L., & Carpenter, P. W. (2003). *Aerodynamics for Engineering Students*. Fifth edition, Elsevier.
4. Lan, E. C. T., & Roskam, J. (2003). *Airplane Aerodynamics and Performance.* DAR Corp.
5. Sadraey, M. (2009). *Aircraft Performance Analysis.* VDM Verlag Dr. Müller.
6. Anderson, J. D. (1999). *Aircraft Performance and Design*. McGraw-Hill.
7. Roskam, J. (2007). *Airplane Flight Dynamics and Automatic Flight Control, Part I.* DAR Corp.
8. Etkin, B., & Reid, L. D. (1996). *Dynamics of Flight, Stability and Control.* Third Edition, Wiley.
9. Stevens, B. L., & Lewis, F. L. (2003). *Aircraft Control and Simulation*. Second Edition, Wiley.
10. Chemezov, D., et al. (2021). Pressure distribution on the surfaces of the NACA 0012 airfoil under conditions of changing the angle of attack. *ISJ Theoretical & Applied Science, 09 (101)*, 601-606.
11. Chemezov, D., et al. (2021). Stressed state of surfaces of the NACA 0012 airfoil at high angles of attack. *ISJ Theoretical & Applied Science, 10 (102)*, 601-604.
12. Chemezov, D., et al. (2021). Reference data of pressure distribution on the surfaces of airfoils

having the names beginning with the letter A (the first part). *ISJ Theoretical & Applied Science, 10 (102)*, 943-958.
13. Chemezov, D., et al. (2021). Reference data of pressure distribution on the surfaces of airfoils having the names beginning with the letter A (the second part). *ISJ Theoretical & Applied Science, 11 (103)*, 656-675.
14. Chemezov, D., et al. (2021). Reference data of pressure distribution on the surfaces of airfoils having the names beginning with the letter B. *ISJ Theoretical & Applied Science, 11 (103)*, 1001-1076.
15. Chemezov, D., et al. (2021). Reference data of pressure distribution on the surfaces of airfoils having the names beginning with the letter C. *ISJ Theoretical & Applied Science, 12 (104)*, 814-844.
16. Chemezov, D., et al. (2021). Reference data of pressure distribution on the surfaces of airfoils having the names beginning with the letter D. *ISJ Theoretical & Applied Science, 12 (104)*, 1244-1274.
17. Chemezov, D., et al. (2022). Reference data of pressure distribution on the surfaces of airfoils (hydrofoils) having the names beginning with the letter E (the first part). *ISJ Theoretical & Applied Science, 01 (105)*, 501-569.
18. Chemezov, D., et al. (2022). Reference data of pressure distribution on the surfaces of airfoils (hydrofoils) having the names beginning with the letter E (the second part). *ISJ Theoretical & Applied Science, 01 (105)*, 601-671.
19. Chemezov, D., et al. (2022). Reference data of pressure distribution on the surfaces of airfoils having the names beginning with the letter F. *ISJ Theoretical & Applied Science, 02 (106)*, 101-135.
20. Chemezov, D., et al. (2022). Reference data of pressure distribution on the surfaces of airfoils having the names beginning with the letter G (the first part). *ISJ Theoretical & Applied Science, 03 (107)*, 701-784.
21. Chemezov, D., et al. (2022). Reference data of pressure distribution on the surfaces of airfoils having the names beginning with the letter G (the second part). *ISJ Theoretical & Applied Science, 03 (107)*, 901-984.
22. Chemezov, D., et al. (2022). Reference data of pressure distribution on the surfaces of airfoils having the names beginning with the letter G (the third part). *ISJ Theoretical & Applied Science, 04 (108)*, 401-484.
23. Chemezov, D., et al. (2022). Reference data of pressure distribution on the surfaces of airfoils having the names beginning with the letter H (the first part). *ISJ Theoretical & Applied Science, 05 (109)*, 201-258.
24. Chemezov, D., et al. (2022). Reference data of pressure distribution on the surfaces of airfoils having the names beginning with the letter H (the second part). *ISJ Theoretical & Applied Science, 05 (109)*, 529-586.
25. Chemezov, D., et al. (2022). Reference data of pressure distribution on the surfaces of airfoils having the names beginning with the letter I. *ISJ Theoretical & Applied Science, 06 (110)*, 1-7.
26. Chemezov, D., et al. (2022). Reference data of pressure distribution on the surfaces of airfoils having the names beginning with the letter J. *ISJ Theoretical & Applied Science, 06 (110)*, 18-25.
27. Chemezov, D., et al. (2022). Reference data of pressure distribution on the surfaces of airfoils having the names beginning with the letter K. *ISJ Theoretical & Applied Science, 07 (111)*, 1-10.
28. Chemezov, D., et al. (2022). Reference data of pressure distribution on the surfaces of airfoils having the names beginning with the letter L. *ISJ Theoretical & Applied Science, 07 (111)*, 101-118.
29. Chemezov, D., et al. (2022). Reference data of pressure distribution on the surfaces of airfoils having the names beginning with the letter M. *ISJ Theoretical & Applied Science, 10 (114)*, 307-392.
30. Chemezov, D., et al. (2022). Reference data of pressure distribution on the surfaces of airfoils having the names beginning with the letter N (the first part). *ISJ Theoretical & Applied Science, 12 (116)*, 801-892.
31. Chemezov, D., et al. (2022). Reference data of pressure distribution on the surfaces of airfoils having the names beginning with the letter N (the second part). *ISJ Theoretical & Applied Science, 12 (116)*, 901-990.
32. Chemezov, D., et al. (2023). Reference data of pressure distribution on the surfaces of airfoils having the names beginning with the letter O. *ISJ Theoretical & Applied Science, 01 (117)*, 624-635.